

Seismic strain analysis of buried pipelines in a fault zone using hybrid FEM-ANN approach

Seyed Kazem Sadat Shokouhi^{*1}, Azam Dolatshah² and Ehsan Ghobakhloo¹

¹Department of Civil Engineering, Islamic Azad University, South Tehran Branch, Tehran, Iran

²Department of Civil Engineering, Islamic Azad University, Dezful Branch, Dezful, Iran

(Received April 29, 2013, Revised June 05, 2013, Accepted July 11, 2013)

Abstract. This study was concerned on the application of a hybrid approach for analyzing the buried pipelines deformations subjected to earthquakes. Nonlinear time-history analysis of Finite Element (FE) model of buried pipelines, which was modeled using laboratory data, has been performed via selected earthquakes. In order to verify the FE model with experiments, a statistical test was done which demonstrated a good conformity. Then, the FE model was developed and the optimum intersection angle of pipeline and fault was obtained via genetic algorithm. Transient seismic strain of buried pipeline in the optimum intersection angle of pipeline and fault was investigated considering the pipes diameter, the distance of pipes from fault, the soil friction angles and seismic response duration of buried pipelines. Also, a two-layer perceptron Artificial Neural Network (ANN) was trained using results of FE model, and a nonlinear relationship was obtained to predict the bending strain of buried pipelines based on the pipes diameter, intersection angles of the pipelines and fault, the soil friction angles, distance of pipes from the fault, and seismic response duration; whereas it contains a wide range of initial input data without any requirement to laboratory measurements.

Keywords: seismic strain analysis; buried pipelines; finite element method (FEM); genetic algorithm (GA); artificial neural network (ANN)

1. Introduction

The fault motions due to earthquake cause serious hazards to buried pipelines, as an important lifeline, leading to local failure of pipelines which impose considerable economic and environmental losses.

Buried pipelines crossing fault are often damaged in earthquakes due to forces and deformation imposed on them through interactions at the soil-pipe interface. That is, the ground moves and thereby causes the pipe to deform (Zhao *et al.* 2010). Post-earthquake investigations have demonstrated that the majority of seismic damages to continuous oil and gas steel pipelines were caused by Permanent Ground Deformations (PGDs) such as fault movements, landslides, liquefaction-induced lateral spread, whereas only few pipelines were damaged by wave propagation (Liang and Sun 2000). Such pipeline damages have been reported in numerous

* Corresponding author, Engineer, E-mail: shokouhi.eng@gmail.com

earthquakes, such as the 1971 San Fernando earthquake (Jennings 1971), and, more recently, the 1995 Kobe earthquake (Nakata and Hasuda 1995), the 1999 Kocaeli earthquake (EERI 1999) and the 1999 Chi-Chi earthquake (Takada and Hassani 2001).

The principal forms of PGD are surface faulting, land sliding, seismic settlement, and lateral spreading due to soil liquefaction. PGD frequently involves differential ground movement wherein two sides move either horizontally or vertically with respect to each other, across a slip or fault plane (Choo *et al.* 2007). Whether the differential ground movement results in a pipe primarily in tension or compression depends on the relative orientation of the fault and the pipe as well as the direction of faulting. For example, right lateral strike-slip faulting and normal faulting with a negative intersection angle result in axial tension and bending in the pipe. However, thrust faulting and right lateral strike-slip fault with a positive angle results in axial compression and bending (Choo *et al.* 2007). To assess the pipeline strength against an imposed strike-slip fault displacement, the distribution of stress and strain within the pipeline wall should be calculated for the imposed deformation. The work of Newmark and Hall (1975) was among first attempts to predict the pipeline mechanical response under a fault displacement using a simplified analytical model. This model consists of a long cable with small displacements, and relates the soil slip friction on the pipe directly to the earth static pressure. This work was extended by Kennedy *et al.* (1977) and Kennedy and Kincaid (1983) considering the non-uniform friction between the pipe and the surrounding soil. This methodology was enhanced by Wang and Yeh (1985) to account for the pipeline bending stiffness. Also, Mc Caffrey and O'Rourke (1983) and Desmod *et al.*, (1995) studied the development of strains in buried pipes crossing faults based on the performance of gas and water pipes during the San Fernando earthquake. Kokavessis and Anagnostidis (2006) proposed a Finite Element Method (FEM) to simulate buried pipeline behavior under permanent ground-induced actions, using contact elements to describe the soil-pipe interaction. Furthermore, an analytical methodology was presented by Karamitros *et al.* (2007), which introduced a number of refinements in the existing methodologies. Liu *et al.* (2008) conducted a numerical simulation of pipelines crossing active faults through a shell Finite Element (FE) model, similar to the model by Karamitros *et al.* (2007) (i.e. a combination of shell elements and springs). Choo *et al.* (2007), Ha *et al.* (2008) and Abdoun *et al.* (2009) undertook laboratory studies based on centrifuge modeling for investigating buried pipelines subject to deformation due to faulting. Considering the effect of rupture, thickness and backfill cover rigidity of pipelines, Zhao *et al.* (2010) analyzed the pipe response to ground movement by using a three dimensional (3D) nonlinear FEM and acquired strain values toward distance from fault in the plastic state. Joshi *et al.* (2011) investigated buried pipelines subjected to reverse fault motion using a FE model. They found that the pipeline's capacity to accommodate reverse fault offset can be increased significantly by choosing a near-parallel orientation in plan with respect to the fault line.

Some studies on the seismic optimization of buried pipelines using Genetic Algorithm (GA) have been reported by researchers. Goldberg and Kuo (1987) studied the GAs into the pipeline optimization. In the mentioned research, the mechanics, power, and application of a GA in the approximate solution of a pipeline engineering optimization problem have been examined. Li *et al.* (2008) proposed the GA for seismic topology optimization of lifeline network systems. They attempted to find the least-cost network topology while the seismic reliability between the sources and each terminal satisfies prescribed reliability constraints. Liu *et al.* (2012) presented the algorithms for seismic topology optimization of water distribution network. To do this, two investment importance indexes, i.e., a pipeline investment importance index and a diameter investment importance index, were introduced to evaluate the contribution of element to the

network. Then, different optimization algorithms were defined to solve the optimization model. The Artificial Neural Network (ANN) has been used to predict the seismic behavior of buried pipelines. Sinha and Fieguth (2006) proposed neuro-fuzzy network for the classification of buried pipe defects. They introduced a new neuro-fuzzy classifier that combines neural networks and concepts of fuzzy logic for the classification of defects by extracting features in segmented buried pipe images. Moghaddas Tafreshi *et al.* (2007) performed the analysis of buried plastic pipes in reinforced sand under repeated-load using neural network and regression model. The ANN and regression model for predicting the vertical deformation of high-density polyethylene pipes, subjected to repeated loadings to simulate the heavy vehicle loads, have been investigated. Roudsari and Hosseini (2011) employed the ANN for reliability assessment of buried steel pipeline networks subjected to earthquake wave propagation.

Herein, seismic strains in High Density Polyethylene (HDPE) buried pipelines subjected to seismic waves are analyzed using a hybrid approach in the present study. To do this, a FE model, by which soils surrounding the pipeline are modeled via nonlinear springs that support the pipeline at discrete points, is modeled using 3D beam elements. Then, the Nonlinear Time-history Analysis (NTA) is performed to evaluate the seismic response of buried pipelines. This way, FE results are statistically verified with laboratory data performed by Choo *et al.* (2007). After that, the numerical model is developed in which the intersection angle of the pipelines and fault is optimized using GA and the transient seismic strains of buried pipelines are investigated considering the pipes diameter, the distance of pipes from the fault, the soil friction angles, and the seismic response duration of buried pipelines. Eventually, several ANNs are trained using those developed FE results, and a nonlinear relationship is consequently obtained for the calculation of seismic bending strain.

2. FE model of HDPE buried pipeline

2.1 Soil-pipe interaction

The surrounding soil is of greater stiffness than the flexible pipe and of lesser stiffness than the rigid pipe. For thermoplastic flexible pipes, soil stiffer than the pipe settles less than the pipe displaces, thereby permitting development of soil abutments, a necessary condition for the formation of a soil “arch” (Laster 2007).

Soil properties representative of the backfill should be used to compute axial soil spring forces. Other soil spring forces should generally be based on the native soil properties. Backfill soil properties are appropriate for computing horizontal and upward vertical soil spring forces. It is possible when the extent of pipeline movement relative to the surrounding backfill soil is not influenced by the soils outside the pipe trench. The expressions for maximum soil spring force are based on laboratory and field experimental investigations on pipeline response. The maximum soil spring forces and associated relative displacements which are necessary to develop these forces are computed using the following equations. The maximum axial soil force per unit length of pipe (T_u) transmitted to the pipe is defined as Eq. (1) (ALA-ASCE 2001).

$$T_u = \pi D \beta k + \pi D H \bar{\gamma} \frac{1 + K_0}{2} \tan \delta \quad (1)$$

where (D), (k), (H), ($\bar{\gamma}$), and (K_0) are pipe outside diameter, soil cohesion representative of the soil backfill, depth to pipe centerline, effective unit weight of soil, and coefficient of pressure at rest, respectively. Also, (δ) is interface angle of friction for pipe and soil which is equal to ($f\phi$). However; (ϕ) is internal friction angle of the soil and (f) is coating dependent factor relating to the internal friction angle of the soil to the friction angle at the soil-pipe interface (approximately equal to 0.6 for polyethylene). In addition; (k) is in ksf or $kPa/100$ and adhesion factor (β) is computed using Eq. (2) (ALA-ASCE 2001)

$$\beta = 0.608 - 0.123k - \frac{0.274}{k^2 + 1} + \frac{0.695}{k^3 + 1} \quad (2)$$

The maximum lateral soil force per unit length of pipe (P_u) transmitted to the pipe is defined as Eq. (3) (ALA-ASCE 2001)

$$P_u = N_{ch}kD + N_{qh}\bar{\gamma}HD \quad (3)$$

where (N_{ch}) is the horizontal bearing capacity factor for clay (0 for (k) = 0) and (N_{qh}) is the horizontal bearing capacity factor (0 for (ϕ) = 0°). They are computed using Eq. (4).

$$N_{ch} = q + ux + \frac{v}{(1+x)^2} + \frac{j}{(1+x)^3} \leq 9.0, \quad N_{qh} = q + ux + vx^2 + jx^3 + ex^4 \quad (4)$$

where (x) depends on the ratio of depth to diameter of the pipe. Also (q), (u), (v), (j) and (e) are the coefficients demonstrated in American Lifeline Alliance (ALA-ASCE) guideline (ALA-ASCE 2001).

The maximum vertical bearing soil force per unit length of pipe (Q_d) transmitted to the pipe is defined as Eq. (5) (ALA-ASCE 2001).

$$Q_d = N_c k D + N_q \bar{\gamma} H D + N_\gamma \frac{D^2}{2} \gamma \quad (5)$$

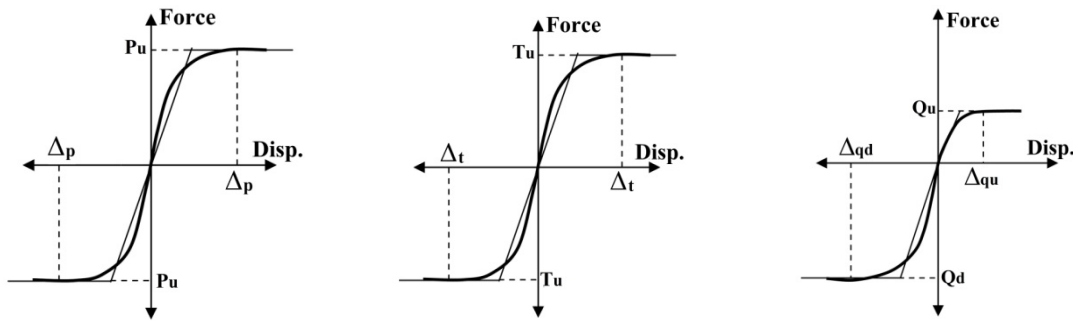
where (γ) is the total unit weight of soil and (N_c), (N_q), (N_γ) are bearing capacity factors obtained using Eqs. (6) and (7), whereas (ϕ) value is based on degree (ALA-ASCE 2001).

$$N_c = \left[\cot(\phi + 0.001) \left\{ \exp[\pi \tan(\phi + 0.001)] \tan^2 \left(45 + \frac{(\phi + 0.001)}{2} \right) - 1 \right\} \right] \quad (6)$$

$$N_q = \exp(\pi \tan \phi) \tan^2 \left(45 + \frac{\phi}{2} \right), \quad N_\gamma = e^{(0.18\phi - 2.5)} \quad (7)$$

The soil-pipe interaction was modeled via the nonlinear Winkler Foundation model in which the interactive behavior has been represented by nonlinear discrete soil springs. The arrangement of spring elements and distribution of their stiffness around the pipe's circumference is of significant importance. In any circumstances, the summation of the soil spring stiffness per unit length along the pipeline should be equated to the corresponding value for the beam spring model. Nonlinear force-displacement properties of springs per unit length of the pipe in three directions (transverse

horizontal, axial and transverse vertical) are illustrated in Fig. 1 (ALA-ASCE 2001). In Fig. 1, (Q_u) indicates the maximum vertical upward soil bearing capacity. Also, (Δ_p), (Δ_t), (Δ_{qd}), and (Δ_{qu}) are the horizontal displacement to develop (P_u), axial displacement to develop (T_u), vertical displacement to develop (Q_d), and vertical displacement to develop (Q_u), respectively.



(a) transverse horizontal spring (b) axial spring (c) transverse vertical spring

Fig. 1 Force-deformation relationships for the soil springs: (a) for transverse horizontal spring, (b) for axial spring, and (c) for transverse vertical spring (ALA-ASCE 2001)

2.2 FE modeling procedure

The considered cases in the laboratory model by Choo *et al.* (2007); pipe cross-section with outer diameter (D) 0.408 m and wall thickness (t_w) 24 mm were chosen for modeling. Pipe properties were assumed based on American Water Works Association (AWWA 2007) guideline. The top of the pipeline was assumed to be buried under 1.124 m of dense sand with friction angle, $\phi = 40^\circ$ and dry unit weight, $\gamma_d = 14.7 \text{ t/m}^3$. A value of 1.55 for coefficient of uniformity was adopted for the soil-pipe interaction. Moreover, intersection angles of the pipeline and fault (α) were considered -85° and -63.5° respectively. Initially, all required and essential parameters for finite element modeling of the buried pipeline were derived from the laboratory model (Choo *et al.* (2007)). Then, the FE model validated and also developed in which the most effective parameters were considered for a high accurate model as well as obtaining the optimum intersection angle of pipeline and fault, and a nonlinear relationship to predict the bending strain of buried pipelines. In the current study, the live load over the ground surface was ignored and also the effect of internal pipe pressure was neglected since the pipeline modeled using beam elements.

The structural response of the HDPE pipeline under PGD is numerically examined using advanced computational techniques. In FE models, a pipe can be discretized using beam elements, and the soil can be connected to the beams as discrete springs with elasto-plastic force-displacement curve, in vertical, transverse, and longitudinal directions. To do this, FE software (ABAQUS 2010) has been utilized to simulate the mechanical behavior of the HDPE buried pipelines, the surrounding soil and their interaction in a rigorous manner, considering the nonlinear geometry of the soil-pipe interaction. The pipeline was modeled using linear beam elements (B31 in ABAQUS) in space. The FE formulation for this element is based on

Timoshenko's beam theory and takes into account transverse shear deformations (ABAQUS 2010). A 17 m straight pipe was considered to be analyzed by the FEM. The entire length of the pipeline was divided into five regions as different blocks for the mesh generation process. Element sizes were identical over each region. The recommendations of ALA-ASCE guideline (2001) were considered for achieving the convergence of FE model. The third region, including the fault crossing point with total length of 1 m (0.5 m on each side of the fault crossing point), has the smallest element size of 0.04 m. The element size comes to 0.08 m at the second and fourth regions beginning at the ends of both sides of the third region and prolonging to 0.2 m (half of the pipe diameter). Figs. 2 and 3 show the geometry section adopted for the presented FE model and connection details of nonlinear soil springs and the pipeline.

Soil surrounding the pipeline was modeled by discrete nonlinear springs. These springs simulated the components of soil-pipe interaction in the axial, transverse horizontal, and transverse vertical directions. The soil springs were modeled using connector elements (CONN3D2 in ABAQUS) between pipe-nodes and corresponding ground nodes (ABAQUS 2010). All the connector elements were associated with axial connector sections, which generate spring forces only in the local axial direction of the element. According to ALA-ASCE (2001), rationale behind

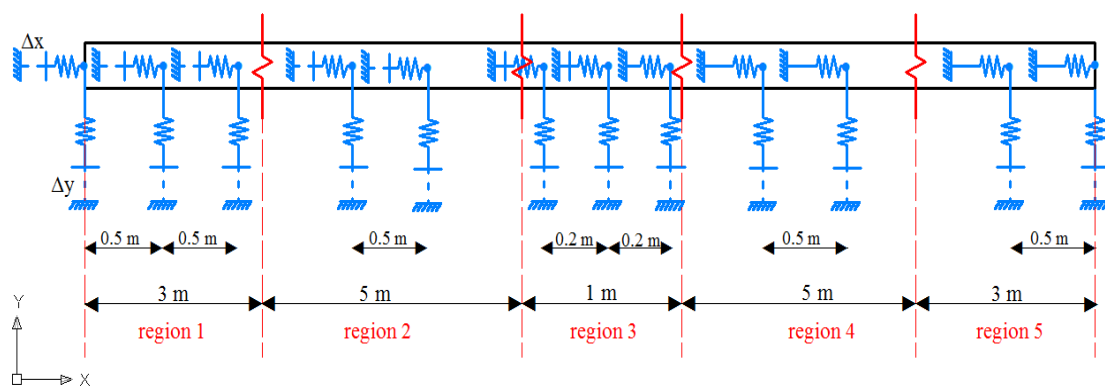


Fig. 2 The geometry adopted for the presented FE model

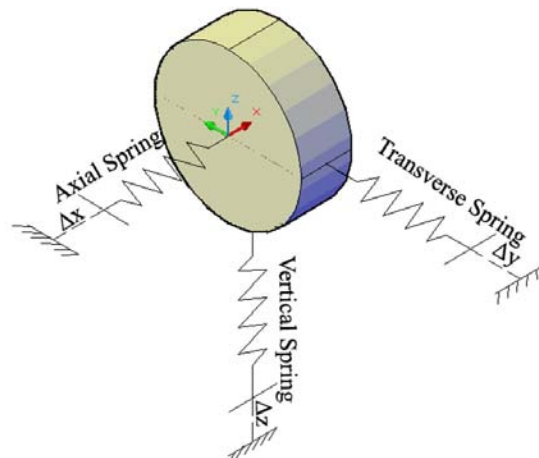


Fig. 3 Connection details of nonlinear soil springs and the pipeline

the present classification lies in the use of Mohr-Coulomb failure criterion employed as nonlinear discrete soil springs of Winkler Foundation model methodology.

For each soil spring, an elastic-perfectly plastic force-deformation relationship was assumed and expressions for the same were adopted from the ALA-ASCE guideline (2001). The equivalent stiffness of these springs depends on the pipe diameter and soil specifications include density, internal friction angle, cohesion coefficient as well as the burial depth of the pipe. Table 1 presents the equivalent stiffness and corresponding displacement of translational nonlinear soil springs in this study. The mentioned soil specifications in Table 1, calculated using Eqs. (1) to (7) and proposed by ALA-ASCE guideline (2001), corresponded to pipes used in the experimental model (Choo *et al.* (2007)).

For a pipeline subjected to PGD, a certain length of the pipeline on either side of the fault crossing point is expected to undergo material yielding due to development of large bending moments (in x-y, x-z and y-z planes) and axial compressive force. The nonlinearity was considered by modeling the pipeline as the elasto-plastic material. The modulus of elasticity, as it is commonly referred to visco-elastic materials, is the ratio between the change in strain and the change in stress levels. This modulus is high initially, but then begins to decrease. The pipe appears to require less force over time to maintain the same strain level. If the material behaves according to elastic principles, it can be described as losing strength. However, polyethylene is visco-elastic and the conclusion that the material is losing strength would be erroneous. The material properties of the HDPE pipe derived from the AWWA guideline (AWWA 2007) are summarized in Table 2. In Table 2, the value of friction coefficient (*f*) has been extracted from ALA-ASCE guideline (2001).

To do Finite Element Analysis (FEA), the appropriate earthquake ground motion was selected considering the proposed offset rate (0.318 m/s) and in a way that the selected earthquake should contain the presented Peak Ground Velocity (PGV) or offset rate by Choo *et al.* (2007). The accelerogram record of Chi-Chi earthquake (1999) was employed to do NTA procedure. The results of NTA and laboratory data using a statistical test were then compared and also verified.

Table 1 Equivalent stiffness and corresponding displacement of translational nonlinear soil springs

Parameters	D = 40 cm	D = 60 cm	D = 80 cm	D = 105 cm
Equivalent stiffness – Axial (N/mm) –	22.8	29.7	38.6	46.7
Displacement (Δ_r -mm)	3	3	3	3
Equivalent stiffness – Transverse (N/mm) –	221	281.3	341.4	393.5
Displacement (Δ_p -mm)	53	67	96	144.6
Equivalent stiffness – Vertical (N/mm) –	859.4	947.1	1224.2	1291.4
Displacement (Δ_{qd} -mm)	40	60	80	105

Table 2 The material properties of selected HDPE pipeline (For prototype scale)

Modulus of elasticity (GPa)	Ultimate tensile strength (MPa)	Outer diameter (mm)	Thickness (mm)	Unit weight (t/m ³)	Friction coefficient <i>f</i>
0.80	15	408	24	14.70	0.60

2.3 NTA procedure of HDPE buried pipeline

2.3.1 Proposed offset rate

As previously mentioned, Choo *et al.* (2007) performed their laboratory tests using the centrifuge modeling through the application of an offset rate equals to 0.318 m/s. Therefore, the proposed offset rate or PGV has been utilized in order to NTA procedure of the proposed FE model.

2.3.2 Selection of proper earthquake ground motion

To do NTA procedure according to a predefined offset rate, an earthquake ground motion that included the proposed PGV was found. For finding such an earthquake, the Pacific Earthquake Engineering Research strong motion database has been utilized (<http://peer.berkeley.edu/smcat>). After searching procedure, the Chi-Chi, Taiwan earthquake (1999) was selected. The input ground motions employed in the following NTA is the accelerogram recorded at the ground of the Taiwan city at the CWB TCU010 station during the Chi-Chi earthquake in 1999. After FE model validation, more earthquakes have been chosen for NTA (in developed models) whose details are shown in Table 3.

2.4 Validation of FE model

In order to validate the numerical modeling according to the laboratory research of Choo *et al.* (2007), the FE models of the HDPE buried pipelines were analyzed using NTA procedure. Indeed, the FE model will be investigated to match the benchmark experiment of Choo *et al.* in the validation procedure.

Although, there are many comparing methods, but one of the most precise methods is the statistical one.

Table 3 The used seismic ground motion records

Earthquake	Record ID	Magnitude (Ms)	PGA (g)	PGV (m/s)	Site classification (USGS)
Chi-Chi (1999)	P1406	7.6	0.088	0.318	B
Imperial Valley (1979)	P0177	6.9	0.519	0.469	C
Kocaeli (1999)	P1096	7.8	0.358	0.464	C
Landers (1992)	P0873	7.4	0.818	0.459	A

In this regards, as an additional more precise validation process, it has been tried to compare experiments and FE results with each other for a better understanding. In terms of comparing two groups of data statistically, the null hypothesis (H_0) is usually a hypothesis of “non- difference”. It means that there is no difference between the ranked of the two comparing groups. These two groups can be defined as laboratory and FE results. When computing the value of Mann-Whitney U test, number of comparisons equals to the product of the number of data in the first group (N_A) times the number of data in the second group (N_B), which equals to $N_A \times N_B$. If the null hypothesis is true, then the value of Mann-Whitney U test should be about half that value. The smallest

possible value of Mann-Whitney U test is zero. The largest possible value equals to $(N_A \times N_B)/2$. If this value is much smaller than that, the P-value will be small. The P-value or calculated probability is the estimated probability of rejecting the null hypothesis of a study question when that hypothesis is true, while the significance level usually is considered as $\lambda = 0.05$. So, if the P-value is more than 0.05, the null hypothesis will be true, especially when P-value is more close to 1. Also, the null hypothesis is true when $RS1 \leq \text{Wilcoxon } W \leq RS2$. Here, RS1 is sum of ranks for the first group and RS2 is sum of ranks for the second group. Similarly, the null hypothesis will be true if $|Z| \leq Z_0$, while Z_0 is the critical value extracted from the Z-distribution graph statistically. This value for the present study equals to 1.96.

3. Optimum intersection angle of the pipeline and fault (α)

3.1 Genetic algorithm

To find the optimal solution for the objective function that is given in the section 5.2, GA is used. GA is well known due to its simplicity and robustness in solving complex problems (Goldberg 1989), and also because of its characteristics, it is suitable for solving problems. This approach makes the optimization computation simpler in comparison with other optimization algorithms. The length of an individual chromosome depends on the number of the intersection angles of the pipeline and fault, whereas all the integer numbers in a chromosome should be unique. GAs are global probabilistic search algorithms inspired by Darwin's survival-of-the-fittest theory. A distinguishing characteristic of GAs is that the algorithms work with codes of the parameter set, not the parameters themselves and generally, the binary coding method is used. When performing the optimization via GA, certain parameters are required such as; population, fitness function, selection, crossover method, mutation, and fitness value. GAs operates on a number of potential solutions, called a population, consisting of some encoding of the parameter set simultaneously. Typically, a population is composed of some individuals which each individual in the population should meet the constraint. The fitness function basically determines which possible solutions get passed on to multiply and mutate into the next generation of solutions. This is usually done by analyzing the "genes" which hold some data about a particular solution to the problem you are trying to solve. Selection is the process of determining the number of times, or trials, a particular individual are chosen for reproduction and, thus, the number of offspring that an individual will produce (Chipperfield *et al.* 1994). In this study, the Roulette Wheel Selection (RWS) scheme is used. RWS is a mechanism to probabilistically select individuals based on some measure of their performance. The basic operator for producing new chromosomes in the GA is that of crossover. The crossover is the operator that produces new individuals (offspring) by exchanging bits of some randomly selected individuals (parents). In GAs, mutation is randomly applied with low probability, typically in the range 0.001 and 0.01, and modifies elements in the chromosomes. The role of mutation is often seen as providing a guarantee that the probability of searching any given string will never be zero and acting as a safety net to recover good genetic material that may be lost through the action of selection and crossover (Goldberg 1989). With mutation, one or more bits are randomly chosen from the individuals and are changed into a different symbol (Guo *et al.* 2004). Fitness values are derived from objective function values through a scaling or ranking function.

In this optimization method, information about the problem, such as the variable parameters, is coded into a genetic string that is known as chromosome (individual). Each of these chromosomes

has an associated fitness value usually determined by the objective function to be maximized or minimized. Each chromosome contains substrings that are known as genes, which contribute in different ways to the fitness of the chromosome (Guo *et al.* 2004). Fig. 4 briefly illustrates the procedures of the GA.

4. Artificial neural network (ANN)

4.1 Feed forward-multilayer neural network

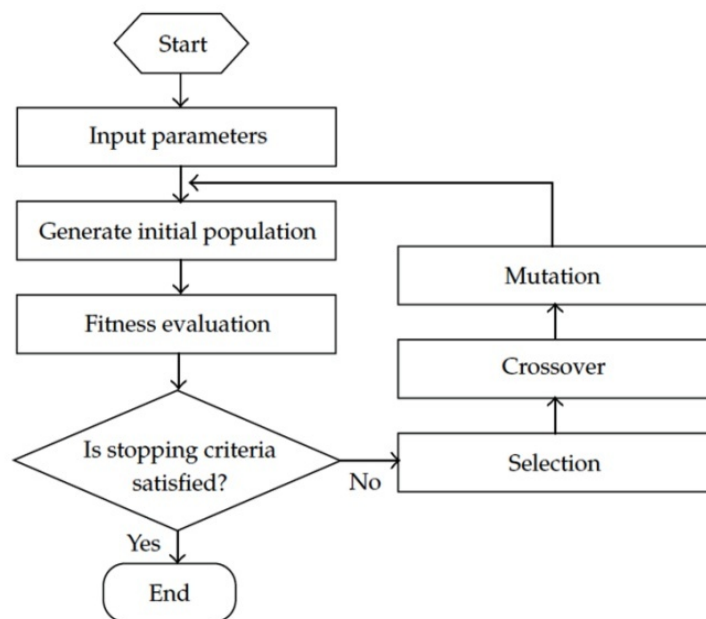


Fig. 4 Flowchart of the GA process (Yi *et al.* 2011)

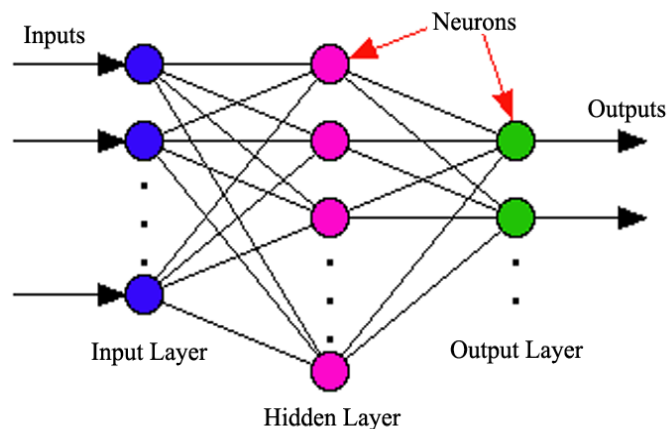


Fig. 5 A schematic ANN and its details (Dawson *et al.* 2000)

The most common neural network includes the feed forward-multilayer networks including one or several hidden layers located between input and output layers. The output of a layer acts as an input for the next layer (Cheung and Cannons 2002). The layers have relations (synaptic joints) serially (fully or partly adjoined) with a feed forward method and there is no joint among units in an equal layer (Jain *et al.* 1996). A feed forward-multilayer network including input neurons, neurons at the first hidden layer, neurons at the second layer, and neurons at the output layer (Rajasekaran and Vijayalakshmi 2007). If the layers of a multilayer network have sigmoid neurons, then the outputs of the network are limited to a small range. As an alternative, the Tansig and Purelin linear functions can be used (Howard and Mark 2006). In this study, a network is used with two layers consisting of the Tansig and Purelin functions in the first and second layers respectively. Fig. 5 illustrates an ANN with a hidden layer, joints among neurons, and the other details (Dawson *et al.* 2000).

4.2 Neural network learning

In this study, the data concerning the diameter of the pipe (D) in meter, the intersection angles of the pipelines and fault (α) in degree, the soil friction angles (ϕ) in degree, the distance of the pipe from the fault (l) in meter, and the seismic response duration (t) are defined as the inputs, and also the transient bending strain values are defined as the targets, creating a nonlinear relationship between the input and target data. In this process, the number of neurons in the input layer is changed and one neuron in the output layer is held constant.

After normalization process of all data, 10% of them were considered as testing data. The remaining 90% data were divided into two groups of validation and training data, while 10% of them were validation and the others were training data.

The training, validation, and testing procedures can be directly performed using ANN toolbox in MATLAB (Howard and Mark 2006). But, authors would prefer doing the testing procedure by a manual written m-file rather than using the ANN toolbox (Howard and Mark 2006), in order to be more conservative. Indeed, testing data will be imported into the m-file containing the calculation related to the developed nonlinear relationship (see Eq. (11)) just after the training and validating networks by MATLAB.

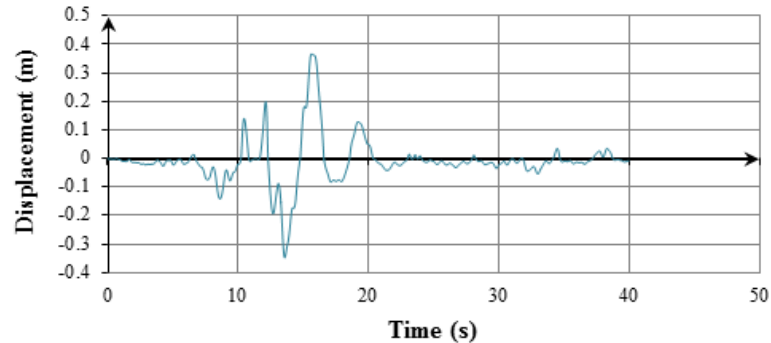
Attaining to the ideal response of the training procedure is based on the validation procedure as well as achieving to an appropriate Mean Squared Error (MSE) which is corresponding to Eq. (8), and also 10000 epochs (Howard and Mark 2006).

$$Mse = \frac{1}{N} \sum_{i=1}^N (y_i - \bar{y})^2 \quad (8)$$

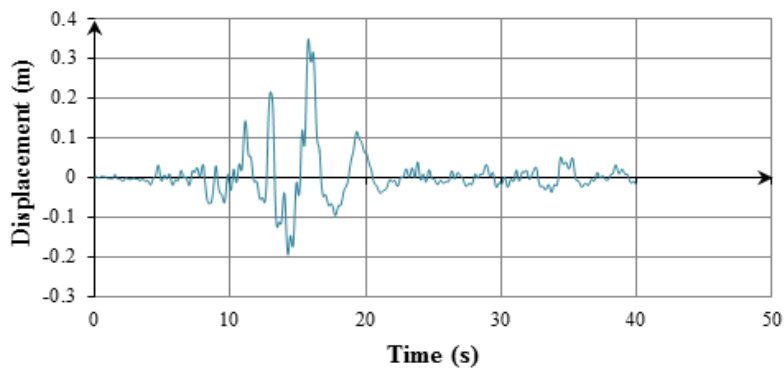
where \bar{y} and (y_i) are the mean value of the data and results of the ANN respectively, and (N) is the number of data. Given the abilities of the feed forward networks for modeling of the nonlinear processes, the multilayer perception network based on back propagation learning algorithm has been used.

5. Results

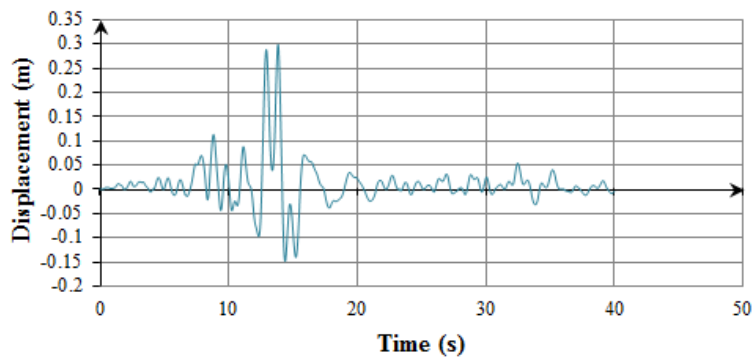
5.1 FEA results based on the laboratory data (prototype FE model)



(a) Axial



(b) Transverse



(c) Vertical

Fig. 6 Displacement time history of the buried pipeline subjected to Chi-Chi earthquake (1999)

As explained before, NTA procedure was performed for the eight FE models. Displacement time history of the buried pipeline subjected to Chi-Chi earthquake (1999) is illustrated in Fig. 6. There is a good conformity between laboratory and NTA results of HDPE buried pipelines. In this regards, Figs. 7(a) and (b) illustrate the results of NTA per $\alpha = -63.5^\circ$ and $\alpha = -85^\circ$ for axial and bending strain under Chi-Chi earthquake (1999), respectively. Given FE results (see Figs. 7(a) and (b)) and the consequence of statistical tests (Table 4) clearly show that there is no significant

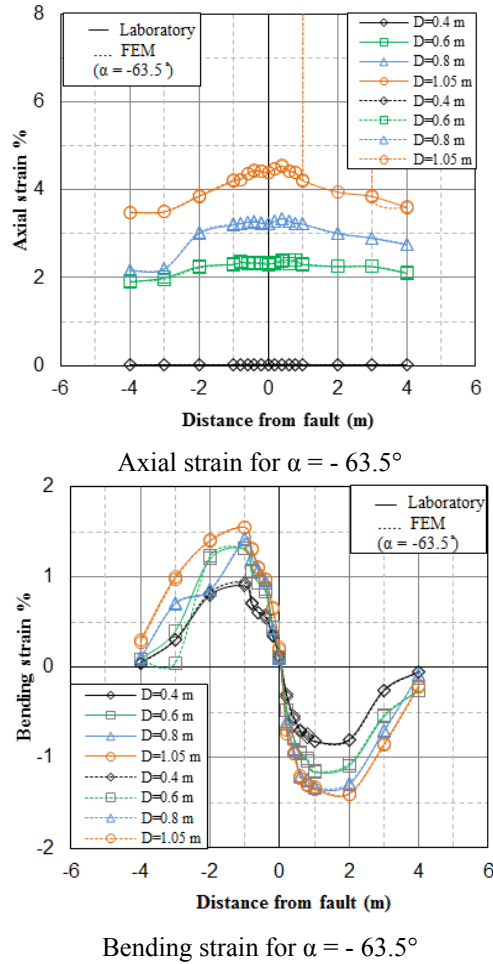


Fig. 7(a) Comparison between FEM and experiment in axial and bending strain results per $\alpha = -63.5^\circ$

difference between laboratory and FE model results. Fig. 8 shows the pipeline buckling of FE models for $\alpha = -63.5^\circ$ and -85° respectively.

5.2 Optimization procedure (obtaining the optimum intersection angle of the pipeline and fault (α))

After FE model verification, the optimum intersection angle of the pipeline and fault (α) has been determined using the GA. For this purpose, the optimum bending strain in the pipes with different diameters were calculated considering pipes diameter, intersection angles of the pipelines and fault, the distance of the pipes from fault, the seismic response duration of buried pipelines and the soil friction angles. The critical strain (ϵ_{cr}) can be rewritten as follows (Vazouras *et al.* 2010):

$$\epsilon_{cr} = \mu \left(\frac{t}{D} \right) \tag{9}$$

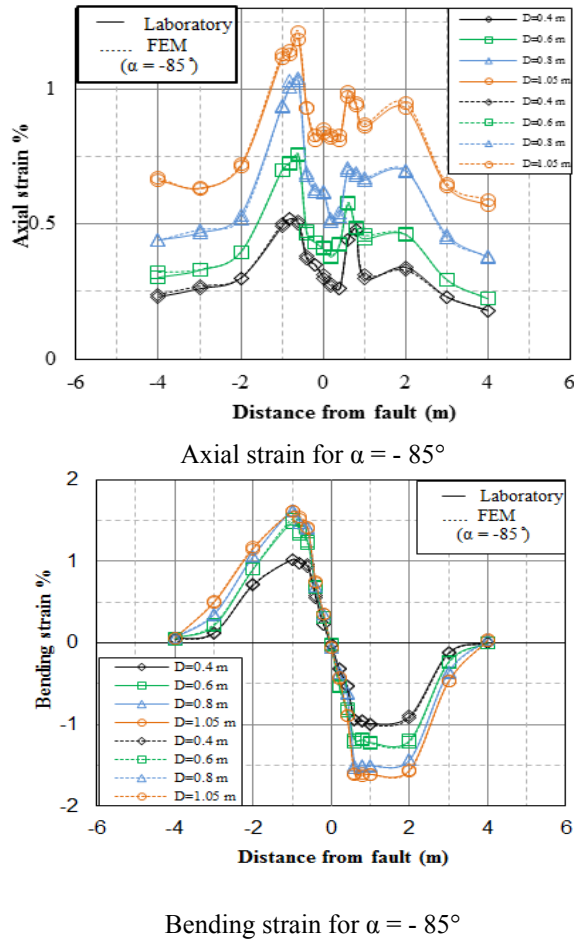


Fig. 7(b) Comparison between FEM and experiment in axial and bending strain results per $\alpha = -85^\circ$

where (μ) is a constant that depends on the pipeline material grade, as well as the amplitude and shape of initial imperfections. Furthermore, the parameters of (t) and (D) are thickness and the outer diameter of the pipe respectively. Eq. (9) demonstrates how to calculate the critical strain in the pipelines. Therefore, this equation can be used as one of the effective parameter in the optimizing. In order to optimize the procedure, Eq. (10) is given as follows:

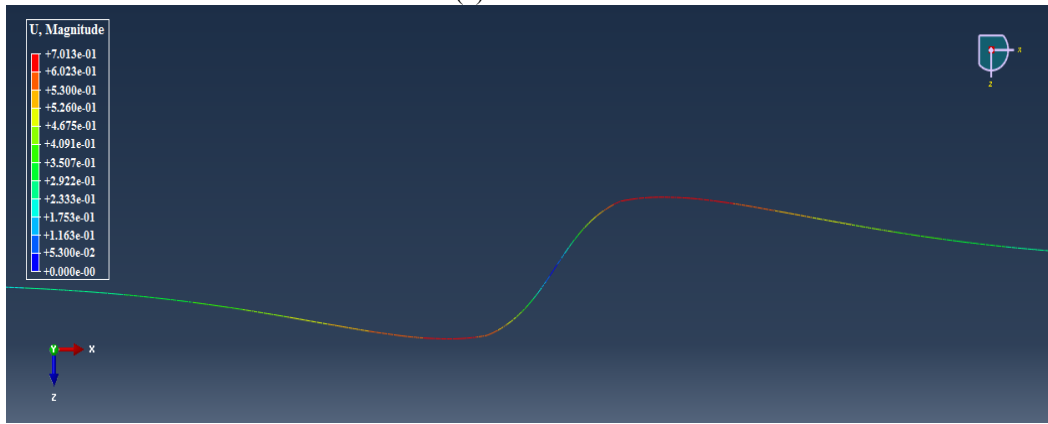
$$\begin{aligned}
 \sum F_i = & \sum_{\alpha=0}^{90} [\sum_{l=-4}^{-2} \sum_{t=0}^{10} [(\sum G(x_1)) + (\sum G(x_2)) + \dots + (\sum (G(x_n)))] + \sum_{l=-2}^0 \sum_{t=10}^{20} [(\sum G(x_1)) + \\
 & (\sum G(x_2)) + \dots + (\sum G(x_n))] + \sum_{l=0}^{+2} \sum_{t=20}^{30} [(G(x_1)) + (G(x_2)) + \dots + (G(x_n))] + \\
 & \sum_{l=+2}^{+4} \sum_{t=30}^{40} [(G(x_1)) + (G(x_2)) + \dots + (G(x_n))]] \\
 G(x_i) = & \epsilon_{cr i} - \epsilon_{FEA i}
 \end{aligned}
 \tag{10}$$

Table 4 Values of Mann-Whitney test for axial and bending strains for comparing FE and laboratory results

Parameter	Comparison results			
	FEM-Lab ($\alpha = -63.5^\circ$, axial)	FEM-Lab ($\alpha = -63.5^\circ$, bending)	FEM-Lab ($\alpha = -85^\circ$, axial)	FEM-Lab ($\alpha = -85^\circ$, bending)
Mann-Whitney U	25.000	15.000	69.000	65.000
Wilcoxon W	116.000	106.000	160.000	156.000
Z	-1.051	-1.045	-0.795	-1.089
P-Value	0.92	0.93	0.91	0.89



(a) $\alpha = -63.5^\circ$



(b) $\alpha = -85^\circ$

Fig. 8 Pipeline buckling of FE models for (a): $\alpha = -63.5^\circ$ and (b): $\alpha = -85^\circ$

In Eq. (10), (F_i) is the fitness function, (ϵ_{FEA_i}) is the strain obtained via FEA, and $G(x_i)$ is the difference between critical and FE strain. Due to the dominant role of the critical strain in the damage evaluation of the pipelines, the prevention of local buckling occurrence in the network, Eq. (10) was proposed as the fitness function in the optimization procedure. This function is minimized by the GA system in the process of evolutionary optimization. In this case study, twelve constraints

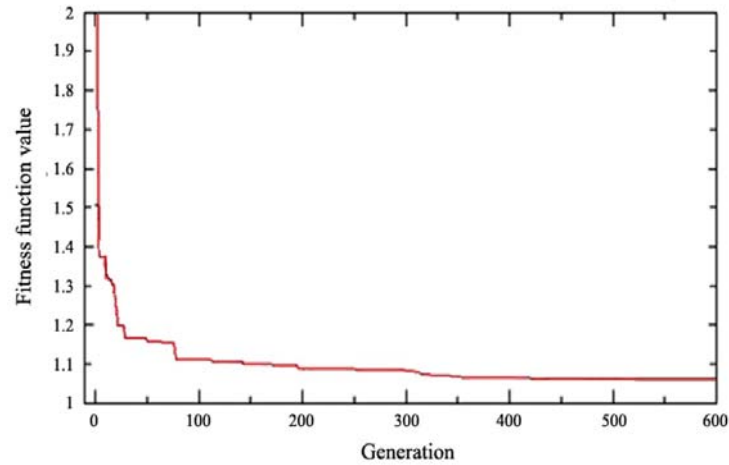


Fig. 9 The evolution progress of the best fitness value of the GA

Table 5(a) Results of optimum values of (ϵ) and (α) parameters in different conditions (loose sand-Kocaeli earthquake 1999)

l (m) t (s)	-4 to -2		-2 to 0		0 to +2		+2 to +4		
	0 to 10		10 to 20		20 to 30		30 to 40		
	ϵ_{Opt} (%)	α_{Opt} ($0 \leq \alpha \leq 90$)	ϵ_{Opt} (%)	α_{Opt} ($0 \leq \alpha \leq 90$)	ϵ_{Opt} (%)	α_{Opt} ($0 \leq \alpha \leq 90$)	ϵ_{Opt} (%)	α_{Opt} ($0 \leq \alpha \leq 90$)	
D (cm)	40	0.81	22.5°	0.97	22.5°	0.67	22.5°	0.61	22.5°
	60	0.92	22.5°	1.23	22.5°	0.84	22.5°	0.72	22.5°
	70	0.98	22.5°	1.39	22.5°	0.89	22.5°	0.78	22.5°
	80	1.08	22.5°	1.61	22.5°	0.96	22.5°	0.87	22.5°
	105	1.33	22.5°	1.97	22.5°	1.18	22.5°	1.03	22.5°

Table 5(b) Results of optimum values of (ϵ) and (α) parameters in different conditions (dense sand-Kocaeli earthquake 1999)

l (m) t (s)	-4 to -2		-2 to 0		0 to +2		+2 to +4		
	0 to 10		10 to 20		20 to 30		30 to 40		
	ϵ_{Opt} (%)	α_{Opt} ($0 \leq \alpha \leq 90$)	ϵ_{Opt} (%)	α_{Opt} ($0 \leq \alpha \leq 90$)	ϵ_{Opt} (%)	α_{Opt} ($0 \leq \alpha \leq 90$)	ϵ_{Opt} (%)	α_{Opt} ($0 \leq \alpha \leq 90$)	
D (cm)	40	0.69	22.5°	0.84	22.5°	0.61	22.5°	0.53	22.5°
	60	0.77	22.5°	1.09	22.5°	0.73	22.5°	0.64	22.5°
	70	0.86	22.5°	1.17	22.5°	0.80	22.5°	0.72	22.5°
	80	0.97	22.5°	1.32	22.5°	0.88	22.5°	0.79	22.5°
	105	1.11	22.5°	1.53	22.5°	1.04	22.5°	0.94	22.5°

and two soil conditions were assigned. Values of GA parameters including crossover individuals, mutation individuals and fitness value are 50, 33, and 1.08, respectively. Fig. 9 shows the evolution progress of the best fitness value of GA. After that, the optimal intersection angle of the pipeline and fault was calculated using the optimum strain results (corresponding values). The optimal strain and intersection angle of the pipeline and fault for loose and dense sands subjected to Kocaeli earthquake (1999) are given in Tables 5 (a) and (b) respectively.

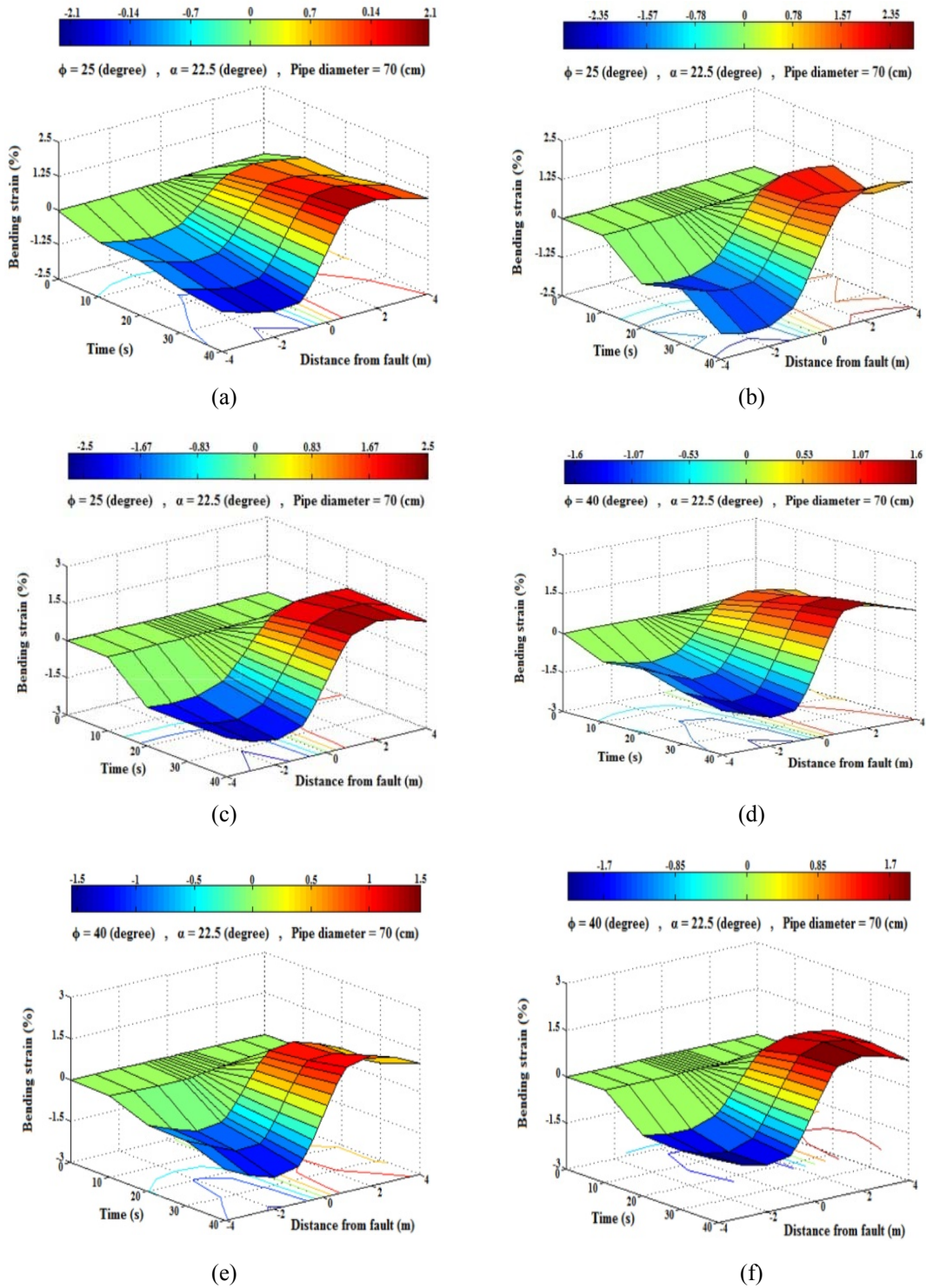


Fig. 10 3D surface plot of transient bending strain obtained using developed FE models for $D = 70$ cm, $\alpha = 22.5^\circ$ and $\phi = 25^\circ$ and 40°

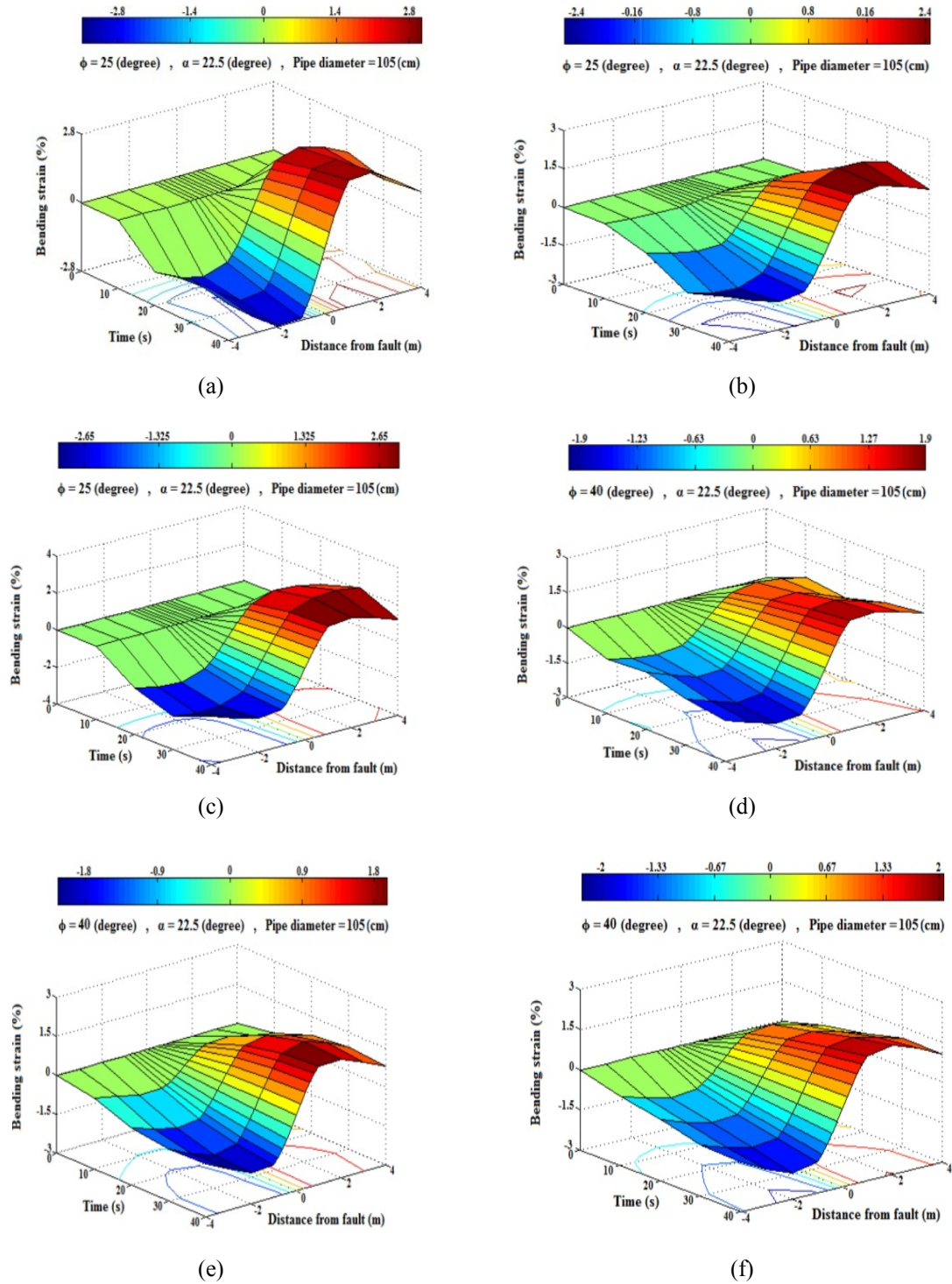


Fig. 11 3D surface plot of transient bending strain obtained using developed FE models for $D = 105$ cm, $\alpha = 22.5^\circ$ and $\phi = 25^\circ$ and 40°

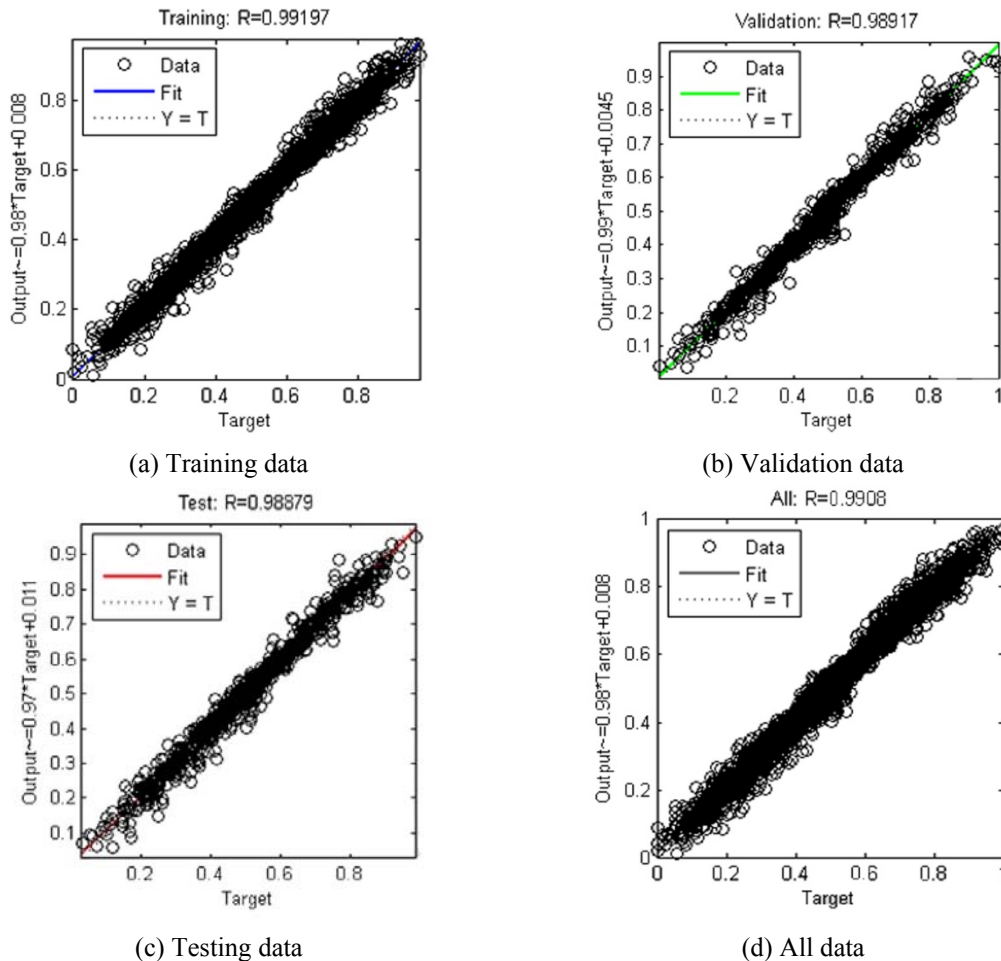


Fig. 12 Regression plot of ANN compared with FEM results

5.3 FEA results using different earthquake ground motions (developed FE models)

After verifying the presented numerical FE model, it has been developed. In the developed numerical models, loose sand with friction angle, $\phi = 25^\circ$ was considered for soil-pipe interaction as well as the dense sand ($\phi = 40^\circ$). Moreover, the effects of distance of the pipes from the fault (l), and the seismic response duration of buried pipelines (t) on the bending strain were investigated in the optimal intersection angle of the pipeline and fault using NTA results. Figs. 10 and 11 show the results of transient bending strain in $\alpha = 22.5^\circ$ considering the distance of pipes from fault ($-4 \leq l \leq 4$) in the loose and dense sands that pipes diameters are equal to 70 and 105 cm at the defined duration ($0 \leq t \leq 40$). The mentioned results demonstrate similar seismic behavior of buried pipelines in comparison with prototype FE model which this matter proves accuracy of developed models.

5.4 ANN results

In order to analyze the bending strains of buried pipeline due to earthquake, learning network structures were trained by employing training data corresponding to FE results. Due to the importance of the bending strain compared with the axial strain; it has been tried to train an ANN to predict the transient bending strain of buried pipelines. Whereas the transient bending strain was considered as the output; the pipes diameter (D), intersection angles of pipelines and fault (α), the soil friction angles (ϕ), distance of the pipes from the fault (l), and seismic response duration (t) were considered as input data.

Totally, there were 5950 series of data containing 595 testing, 536 validation, and 4819 training data. These are entire data used to develop the ANN model.

Appropriate ANNs were trained using training and validation data by MATLAB, and then the best network was selected using the testing procedure. Based on the regression values for training, validation, testing, and all data indicated in Fig. 12; there is no significant difference between FE and predicted ANN results.

Finally, the nonlinear relationship was obtained from training process of the networks, which can be written as Eq. (11).

$$S = w_2 \left(\frac{1 - e^{-2((w_1 \times c) + b_1)}}{1 + e^{-2((w_1 \times c) + b_1)}} \right) + b_2 \quad (11)$$

where (c) is the 5×1 perpendicular vector corresponding to the normalized input data including the pipes diameter (D), intersection angles of pipeline and fault (α), the soil friction angles (ϕ), distance of pipes from the fault (l), and seismic response duration (t). Also, w_1 , w_2 , b_1 and b_2 as weights and biases values which involve constant matrixes obtained in training process, and (S) is the transient bending strain value in the normalized network. All values of bending strain can be estimated using this relationship, even at all mid-points of input data. In other words; this nonlinear relationship obtained using ANN can include a wide range of the input data among the initial input data to calculate related bending strains.

6. Conclusions

Fault crossing buried pipelines subjected to deformation are among the major repercussions of earthquake damaging such systems. In this research, the seismic strain analysis of the buried pipelines was studied using a numerical hybrid FEM-ANN approach. To be specific, the mechanical behavior of HDPE buried pipelines was studied using a simple FE model which utilized 3D beam elements for modeling and nonlinear analysis. The soil-pipe interaction was simulated by associating each pipe-node to a set of three nonlinear springs; however an explicit method using FE software was employed for this nonlinear dynamic analysis. In deed; NTA was performed in order to evaluate the seismic response of buried pipelines. The nonlinearity of the pipe material was considered in the NTA process by which a nonlinear stress-strain curve is connected to the beam elements. After the validation; the FE model was developed to investigate the transient seismic strain of buried pipelines considering the pipes diameter, the distance of the pipes from fault, the soil friction angles, and seismic response duration. A real coded elitist GA with a uniform parent centric crossover operator and a mutation operator was utilized for implementing the optimal intersection angle of the pipeline and fault. Furthermore; this study

evaluated the application of feed forward-multilayer ANN to analyze the HDPE pipelines subjected to earthquake. Hence, the FE results were used as the training data, and then a nonlinear relationship was obtained to predict the bending strain of the buried pipelines. It can be seen that the predicted results confirmed their consistency with the FE results according to regression curves and values. Also, ANN has expanded its results to a predictable wide rang in addition to the FE results. In this study, however, using NTA in FE modeling, and also considering the most effective parameters to pipelines deformation, subjected to earthquake motions in a fault zone, in terms of the optimization procedure of the intersection angle of pipeline and fault in addition to the nonlinear relationship obtained by ANNs can make results more accurate, efficient, and unique.

References

- ABAQUS (2010), ABAQUS user's manual, version 6.10, Simulia, USA.
- Abdoun, T.H., Ha, D., O'Rourke, M.J., Symans, M.D., O'Rourke, T.D., Palmer, M.C. and Stewart, H.E. (2009), "Factors influencing the behavior of buried pipelines subjected to earthquake faulting", *Soil Dyn. Earthq. Eng.*, **29**(3), 415-427.
- American Lifelines Alliance-ASCE (2001), *Guidelines for the design of buried steel pipe*, [with addenda through February 2005], ASCE, USA.
- AWWA (2007), *AWWA Standard for Poly-Ethylene (PE) pressure pipe and fittings*, American Water Works Association, USA.
- Cheung, V. and Cannons, K. (2002), "An introduction to neural networks", University of Manitoba, Manitoba, Canada.
- Chipperfield, A.J., Fleming, P.J., Pohlheim, H. and Fonseca, C.M. (1994), "Genetic algorithm toolbox user's guide", ACSE Research Report No. 512, University of Sheffield, UK.
- Choo, Y.W., Abdoun, T.H., O'Rourke, M.J. and Ha, D. (2007), "Remediation for buried pipeline systems under permanent ground deformation", *Soil Dyn. Earthq. Eng.*, **27**(12), 1043-1055.
- Dawson, C.W., Wilby, R.L., Harpham, C., Brown, M.R., Cranston, E. and Darby, E.J. (2000), "Modeling ranunculus presence in the rivers test and itchen using artificial neural networks", *Proceeding of the 5th Inter'l Conference on GeoComputation*, Greenwich, UK, August.
- Desmod, T.P., Power, M.S., Taylor, C.L. and Lau, R.W. (1995), "Behavior of large-diameter pipeline at fault crossings", *Proceedings of ASCE TCLEE Conference*, San Diego, USA, October.
- Earthquake Engineering Research Institute (1999), Kocaeli: Turkey Earthquake of August 17. EERI, Special Earthquake Report.
- Goldberg, D.E. and Kuo, C.H. (1987), "Genetic algorithms in pipeline optimization", *J. Comp. Civil Eng.*, **1**(2), 128-141.
- Goldberg, D.E. (1989), *Genetic algorithms in search, optimization and machine learning*, Addison-Wesley Pub. Company, Boston, USA.
- Guo, H.Y., Zhang, L., Zhang, L.L. and Zhou, J.X. (2004), "Optimal placement of sensors for structural health monitoring using improved genetic algorithms", *Smart Mater. Struct.*, **13**(3), 528-534.
- Ha, D., Abdoun, T.H., O'Rourke, M.J., Symans, M.D., O'Rourke, T.D., Palmer, M.C. and Stewart, H.E. (2008), "Centrifuge modeling of earthquake effects on buried high-density polyethylene (HDPE) pipelines crossing fault zones", *J. Geotech. Eng. - ASCE*, **134**(10), 1501-1515.
- Howard, D. and Mark, B. (2006), *Neural network toolbox for use with MATLAB. User's guide*, The MathWorks, Inc., USA.
- <http://peer.berkeley.edu/smcat/>
- Jain, A.K., Mao, J. and Mohiuddin, K.M. (1996), "Artificial neural networks: a tutorial", *Computer*, **29**(3), 31-44.

- Jennings, P.C. (1971), "Engineering features of the San-Fernando earthquake February 9, 1971", Earthquake Engineering Research Laboratory, California Institute of Technology Report, Pasadena, California, USA.
- Joshi, S., Prashant, A., Deb, A. and Jain, S.K. (2011), "Analysis of buried pipelines subjected to reverse fault motion", *Soil Dyn. Earthq. Eng.*, **31**(7), 930-940.
- Karamitros, D.K., Bouckovalas, G.D. and Kouretzis, G.P. (2007), "Stress analysis of buried steel pipelines at strike-slip fault crossings", *Soil Dyn. Earthq. Eng.*, **27**(3), 200-211.
- Kennedy, R.P., Chow, A.W. and Williamson, R.A. (1977), "Fault movement effects on buried oil pipeline", *J. Transpo. Eng.*, **103**(5), 617-633.
- Kennedy, R.P. and Kincaid, R.H. (1983), "Fault crossing design for buried gas oil pipelines", *Proceedings of ASME-PVP Conference*, Oregon, USA, June.
- Kokavessis, N.K. and Anagnostidis, G.S. (2006), "Finite element modeling of buried pipelines subjected to seismic loads, soil structure interaction using contact elements", *Proceedings of ASME-PVP Conference*, Vancouver, Canada, July.
- Lester, H.G. (2007), *The Pipe/soil structure-actions and interactions: handbook of polyethylene pipe*, Plastic Pipe Institute, USA.
- Li, J., Liu, W. and Bao, Y. (2008), "Genetic algorithm for seismic topology optimization of lifeline network systems", *Earthq. Eng. Struct. Dyn.*, **37**(11), 1295-1312.
- Liang, J. and Sun, S. (2000), "Site effects on seismic behavior of pipelines: a review", *J. Pressure Vessel Techn. - ASME*, **122**(4), 469-475.
- Liu, M., Wang, Y.Y. and Yu, Z. (2008), "Response of pipelines under fault crossing", *Proc. Inter' Offshore Polar Engi. Conference*, Vancouver, Canada, July.
- McCaffrey, M.A. and O'Rourke, T.D. (1983), "Buried pipeline response to reverse faulting during the 1971 SanFernando Earthquake", *Proceedings of ASME-PVP Conference*, Oregon, USA, June.
- Moghaddas Tafreshi, S.N., Tavakoli Mehrjardi, G. and Moghaddas Tafreshi, S.M. (2007), "Analysis of buried plastic pipes in reinforced sand under repeated-load using neural network and regression model", *Int. J. Civil Eng.*, **5**(2), 118-133.
- Nakata, T. and Hasuda, K. (1995), "Active fault, Hyogoken Nanbu earthquake", *Kagaku*, **65**, 127-42.
- Newmark, N.M. and Hall, W.J. (1975), "Pipeline design to resist large fault displacement", *Proce.U.S. Nat'l Conference on Earthquake Eng.*, Ann Arbor, USA, June.
- Roudsari, M.T. and Hosseini, M. (2011), "Using neural network for reliability assessment of buried steel pipeline networks subjected to earthquake wave propagation", *J. Appl. Sci.*, **11**(18), 3233-3246.
- Sinha, S.K. and Fieguth, P.W. (2006), "Neuro-fuzzy network for the classification of buried pipe defects", *Autom. Constr.*, **15**(1), 73-83.
- Takada, S., Hassani, N. and Fukuda, K. (2001), "A new proposal for simplified design of buried steel pipes crossing active faults", *Earthq. Eng. Struct. Dyn.*, **30**(8), 1243-1257.
- Vazouras, P., Karamanos, S.A. and Dakoulas, P. (2010), "Finite element analysis of buried steel pipelines under strike-slip fault displacements", *Soil Dyn. Earthq. Eng.*, **30**(11), 1361-1376.
- Wang, L.R.L. and Yeh, Y.A. (1985), "A refined seismic analysis and design of buried pipeline for fault movement", *Earthq. Eng. Struct. Dyn.*, **13**(1), 75-96.
- Liu, W., Xu, L. and Li, J. (2012), "Algorithms for seismic topology optimization of water distribution network", *Sci. China Tech. Sci.*, **55**(11), 3047-3056.
- Yi, T.H., Li, H.N. and Gu, M. (2011), "Optimal sensor placement for health monitoring of high-rise structure based on genetic algorithm", *J. Math. Probl. Eng.*, Article ID 395101, 12 pages.
- Zhao, L., Cui, C. and Li, X. (2010), "Response analysis of buried pipelines crossing fault due to overlying soil rupture", *Earthq. Sci.*, **23**(1), 111-116.